Original Article | Thoracic Imaging

https://doi.org/10.3348/kjr.2018.19.1.147
pISSN 1229-6929 · eISSN 2005-8330
Korean J Radiol 2018;19(1):147-152

Korean Journal of Radiology
KJR

Application of Deconvolution Algorithm of Point Spread Function in Improving Image Quality: An Observer Preference Study on Chest Radiography

Kum Ju Chae, MD[1, 2], Jin Mo Goo, MD, PhD[1, 3], Su Yeon Ahn, MD[1], Jin Young Yoo, MD[1], Soon Ho Yoon, MD[1, 3]

[1]Department of Radiology, Seoul National University College of Medicine, and Institute of Radiation Medicine, Seoul National University Medical Research Center, Seoul 03080, Korea; [2]Department of Radiology, Research Institute of Clinical Medicine of Chonbuk National University-Biomedical Research Institute of Chonbuk National University Hospital, Jeonju 54907, Korea; [3]Cancer Research Institute, Seoul National University College of Medicine, Seoul 03080, Korea

Objective: To evaluate the preference of observers for image quality of chest radiography using the deconvolution algorithm of point spread function (PSF) (TRUVIEW ART algorithm, DRTECH Corp.) compared with that of original chest radiography for visualization of anatomic regions of the chest.

Materials and Methods: Prospectively enrolled 50 pairs of posteroanterior chest radiographs collected with standard protocol and with additional TRUVIEW ART algorithm were compared by four chest radiologists. This algorithm corrects scattered signals generated by a scintillator. Readers independently evaluated the visibility of 10 anatomical regions and overall image quality with a 5-point scale of preference. The significance of the differences in reader's preference was tested with a Wilcoxon's signed rank test.

Results: All four readers preferred the images applied with the algorithm to those without algorithm for all 10 anatomical regions (mean, 3.6; range, 3.2–4.0; $p < 0.001$) and for the overall image quality (mean, 3.8; range, 3.3–4.0; $p < 0.001$). The most preferred anatomical regions were the azygoesophageal recess, thoracic spine, and unobscured lung.

Conclusion: The visibility of chest anatomical structures applied with the deconvolution algorithm of PSF was superior to the original chest radiography.

Keywords: *Preference test; Image quality; Digital chest radiography; Modulation transfer function; Deconvolution algorithm; Point spread function*

INTRODUCTION

During recent years, with the rapid development of electronic and computer technology, digital radiographic detectors have undergone considerable investigation and development. There are two main types of flat-panel detectors: direct and indirect type. For the direct detectors, amorphous Selenium (a-Se) converts X-ray energy to electronic charges directed to the collecting pixel capacitors by an electric field (1, 2). For indirect detectors, Gadolinium Oxysulfide (Gadox) or Cesium Iodide (CsI) is used as a scintillator. X-ray signals absorbed by a scintillator convert into light photons that are subsequently detected and stored in the form of electronic charge in the capacitors

Received May 19, 2017; accepted after revision July 19, 2017.
This study was supported by a grant of the Korea Health Technology R&D Project through the Korea Health Industry Development Institute (KHIDI), funded by the Ministry of Health & Welfare, Republic of Korea (grant number : HI15C1532).
Corresponding author: Jin Mo Goo, MD, PhD, Department of Radiology, Seoul National University College of Medicine, and Institute of Radiation Medicine, Seoul National University Medical Research Center, 101 Daehak-ro, Jongno-gu, Seoul 03080, Korea.
• Tel: (822) 2072-2624 • Fax: (822) 743-7418
• E-mail: jmgoo@plaza.snu.ac.kr

associated with each pixel (3, 4). Samei and Flynn (5) reported that the modulation transfer function (MTF) of the direct type detector differs slightly from the ideal function from the effects of fluorescent radiation transport, but the MTF of indirect detection system is reduced because of the blurring of the scattered light from the scintillator, resulting in reduced sharpness. However, the detective quantum efficiency (DQE) is higher in the indirect detection system at frequencies below 2.5 mm^{-1}.

Recently, to reduce the scattering signal from indirect type detectors, a deconvolution algorithm of point spread function (PSF) (TRUVIEW ART, DRTECH Corp., Seongnam, Korea) has been developed. This system may increase sharpness of the image generated by the indirect detector like by a direct type without decrease of the DQE. In a performance study, the MTF of the image with TRUVIEW ART was increased by more than 20% (57.8%) at the 2 lp/mm of spatial frequency compared to original indirect type detector (37.4%) (Supplementary Fig. 1 in the online-only Data Supplement).

The purpose of our study was to compare the image quality of chest radiography with a deconvolution algorithm and that of chest radiography collected with standard protocol for the visualization of anatomic regions of the chest, and to identify if the increased MTF of the algorithm may be potentially applicable in clinical practice.

MATERIALS AND METHODS

Patient Data

This prospectively designed study was approved by our Institutional Review Board and written informed consent was obtained from all participants (D-1609-071-719). From November–December 2016, patient selection criteria included patients that visited our hospital for chest CT and whose age is older than 20 years. Patients with an opacity occupying one-third of the hemithorax or with a history of thoracic surgery were excluded from the study, and a total of 50 participants were included in our study. There were 29 men (58%) and 21 women (42%), and the median age was 57.5 (range, 39–75).

Image Acquisition

Participants underwent chest radiography with the standard posteroanterior (PA) projection. The flat plate detector (Digital Diagnost Ver 4.0; Philips Healthcare, Hamburg, Germany) consisted of an X-ray tube and generator (Philips Healthcare). This system worked with non-automatic exposure control and the X-ray exposure conditions were 117 kVp, 320 mA, and 2.5 mAs using a 180 cm source to image receptor distance and an anti-scatter grid (85 lines per centimeter; ratio, 10:1). Resolution for this detector was 2560 x 3072 pixels with a pixel pitch of 140 μm, leading to an active imaging area 36 x 43 cm. By applying this standard protocol, a chest PA radiograph was obtained from 50 patients. These 50 chest PA raw images from 50 patients were duplicated into 100 images, and the TRUVIEW ART algorithm was applied to these 50 images. Thus, we collected two sets of images per patient with or without TRUVIEW ART algorithm. All images were processed with a standardized postprocessing algorithm supplied by the manufacturer (Econsole1 SW; DRTECH Corp.).

Digital data were sent to a picture archiving and communication system (PACS) server (Infinitt Healthcare, Seoul, Korea) and distributed to workstations. The window width and window level of the images were automatically optimized by the customized program. Readers could adjust brightness and contrast of the images. For this reader preference study, patient identification was replaced by a sequence number on all images. Each pair of images was displayed side-by-side in a random manner.

TRUVIEW ART Algorithm Description

TRUVIEW ART is a technology that improves MTF by restoring blurred regions of the image by using a deconvolution technique that inversely estimates the scatter component generated in the scintillator of the indirect conversion detector. This technology consists of 1) the PSF calibration step to estimate the light scattering form and 2) deconvolution step to conduct actual image restoration using the estimated PSF. The PSF is calibrated by estimating the scattered signal generated by an X-ray

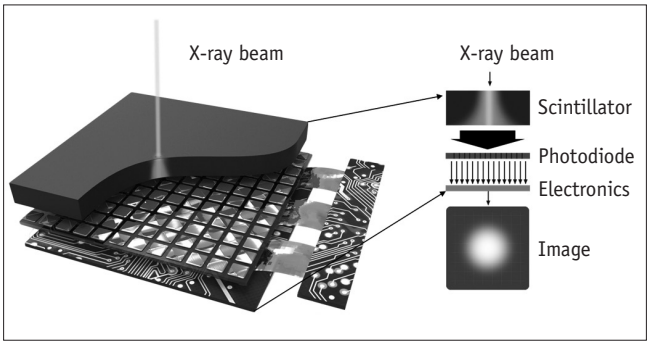

Fig. 1. Process of Gaussian modelling of light scattering in scintillator.

Korean Journal of Radiology
KJR

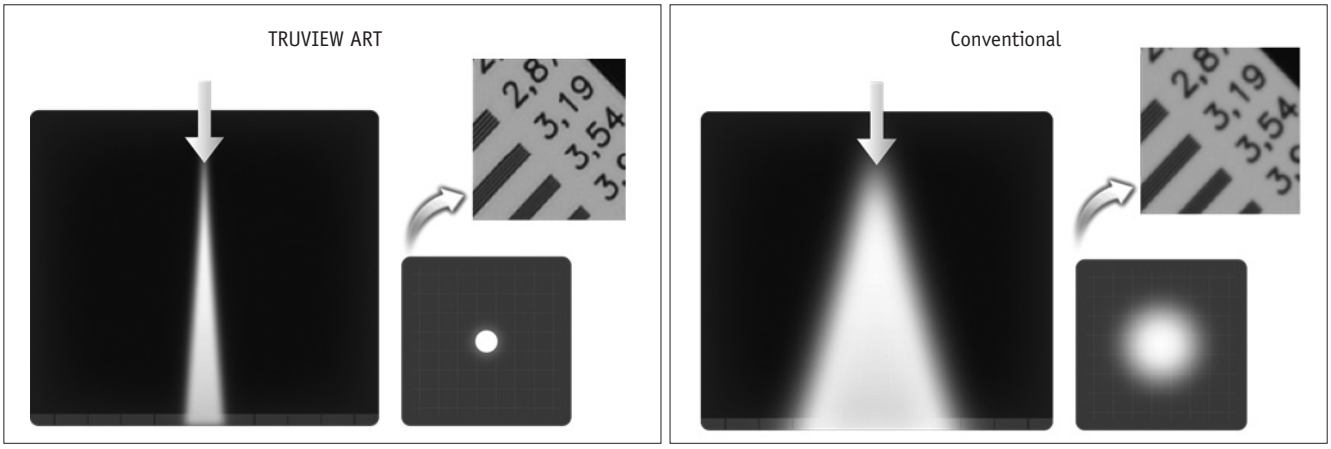

A B

Fig. 2. Reconstructed image with and without TRUVIEW ART (DRTECH Corp.).
A. By elimination of scattering effects applying TRUVIEW ART, blurred image can be seen more clearly. **B.** Without TRUVIEW ART, light scattering occurs by light spread of conventional scintillator, and image looks blurred.

Table 1. Preference Rating between Original and TRUVIEW ART (DRTECH Corp.) Applied Chest Radiography for 11 Anatomical Regions

Anatomical Regions	Preference Rating					Mean Value of Observation Rating	*P*
	1	2	3	4	5		
Unobscured lung	0	14	38	116	32	3.8	< 0.001
Hilum	0	0	81	116	3	3.6	< 0.001
Minor fissure	0	0	151	47	2	3.3	< 0.001
Rib	0	2	91	107	0	3.5	< 0.001
Heart border	0	13	99	88	0	3.4	< 0.001
Retrocardiac lung	0	0	165	35	0	3.2	< 0.001
Subdiaphragmatic lung	0	0	148	50	2	3.3	< 0.001
Azygoesophageal recess	0	0	21	152	27	4.0	< 0.001
Proximal airway	0	0	52	148	0	3.7	< 0.001
Thoracic spine	0	1	33	156	10	3.9	< 0.001
Overall appearance	0	8	24	168	0	3.8	< 0.001

signal when it passes through a scintillator. The scattered signal on the image has a round-shaped PSF that follows a Gaussian model (Fig. 1). These PSFs have different shapes depending on the type and thickness of the scintillator. When the PSF is optimized, it is applied to the following equation in the deconvolution step to finally obtain a clear image (6-8) (Fig. 2).

$I * PSF = B$, $I = B * PSF^{-1}$

I = clear image, B = blurred image, PSF = point spread function, PSF^{-1} = inverse PSF, * = convolution

Image Evaluation

Four chest radiologists (chest radiologists with 5–10 years of experience) compared the paired images independently. Those radiologists did not know about patients' history. Ten anatomical regions and overall appearance were evaluated in the PA views. The anatomical regions included unobscured lung, hilum, minor fissure, retrocardiac lung, lung projected below the diaphragm (subdiaphragmatic lung), azygoesophageal recess, heart border, rib, proximal airway, and thoracic spine. Each of the 11 variables was assigned a five-point ordinal scale: score 1, strongly preferred A; score 2, somewhat preferred A; score 3, no preference; score 4, somewhat preferred B; and score 5, strongly preferred B (A = initial image, B = second image) without knowledge of image protocol or other reader's scores. Because each pair of images was randomly arranged, this score was rearranged to A as the original image and B as the TRUVIEW ART-applied image in describing results.

Statistical Analysis

Mean values were calculated for each anatomic region and each reader. To determine preference for each anatomic regions, Wilcoxon signed rank test was used with five-scale

scores. All statistics were calculated by using statistical software SPSS (SPSS version 16.0; SPSS Inc., Chicago, IL, USA) and *p* value of 0.05 or less was considered statistically significant.

RESULTS

The composite data for all readers and the mean value of the preference rating for each anatomic region are summarized in Table 1. All four readers preferred the images applied with the algorithm to those without algorithm for all ten anatomical regions (mean, 3.6; range of the mean values of 4 interpreters, 3.2–4.0; $p < 0.001$) and for the overall image quality (mean, 3.8; range of the mean values of 4 interpreters, 3.3–4.0; $p < 0.001$).

The algorithm-applied images were most highly preferred in anatomic landmarks of azygoesophageal recess (mean, 4.0) and thoracic spine (mean, 3.9), but least preferred in the retrocardiac lung (mean, 3.2), subdiaphragmatic lung (mean, 3.3), and minor fissure (mean, 3.3). Although the algorithm-applied images were highly preferred in unobscured lungs (mean, 3.8), there was preference for the original images in 7% of observations, the highest among various landmarks.

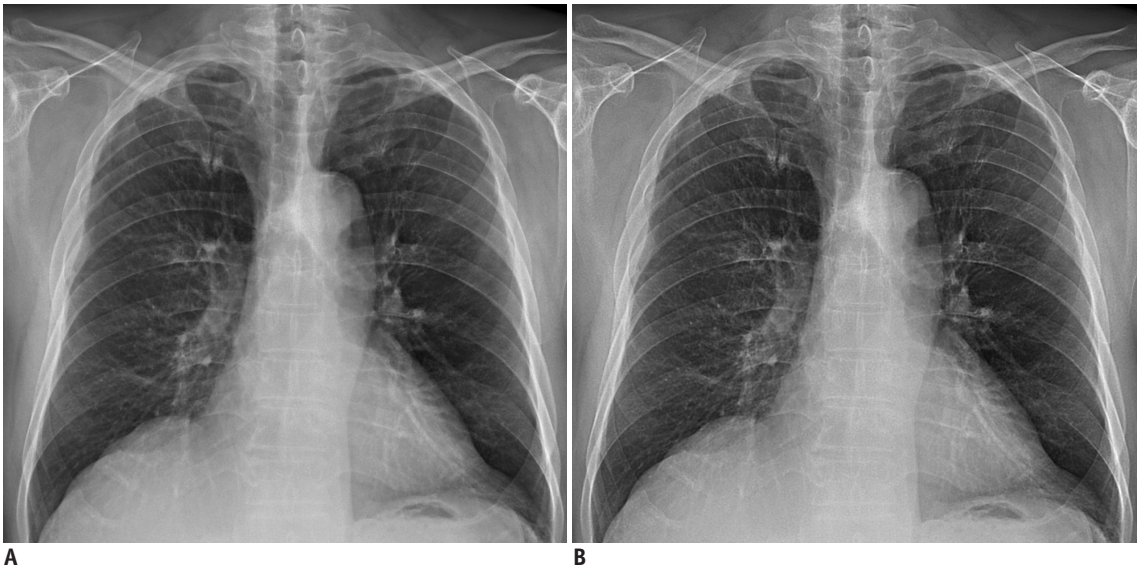

Fig. 3. 75-year-old man with coronary artery disease.
Compared with original chest radiography **(A)**, TRUVEIW ART applied chest radiography **(B)** shows better depiction in overall image quality.

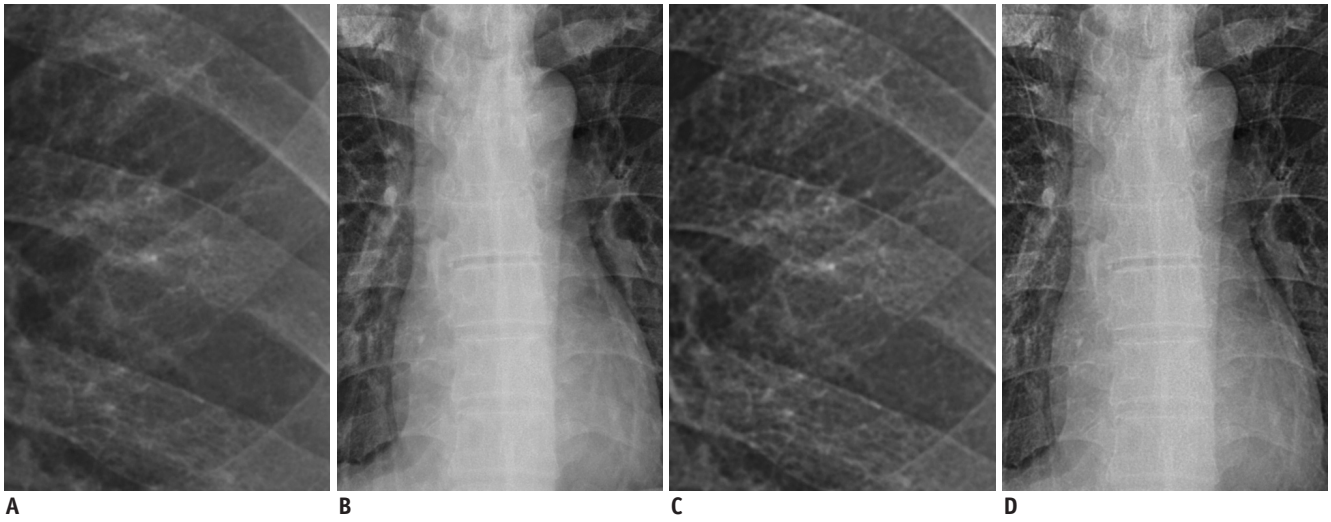

Fig. 4. 61-year-old man with non-small cell lung cancer.
Compared with original chest radiography **(A, B)**, TRUVEIW ART applied chest radiography **(C, D)** shows better visualization of unobscured lung and thoracic spines.

Korean Journal of Radiology
KJR

The subjective image quality rating was satisfactory and no artifacts were observed (Figs. 3, 4).

DISCUSSION

Recently, a virtual grid technique using scatter correction software has been developed to improve image quality by reducing the effect of scattered X-rays (9, 10). In this approach, an iterative estimation of the scatter signal through Monte Carlo simulations of water phantoms is conducted, and scatter correction is conducted by compensating the contrast loss due to scattered signals. It provides image quality comparable to that acquired with grid exposure, with the decreased radiation exposure.

Like the virtual grid technique, the TRUVIEW ART is software eliminating scatters from the image, but the difference is improving the sharpness of the image by restoring the scatter generated in the scintillator inside of the detector. Thus, it eliminates blurring of the image and increases the MTF as well. Therefore, it is possible to achieve a high-resolution image required for fine anatomical structures such as microcalcification, blood vessels, and fracture, that is useful for clinical diagnosis. In addition, this technique restores the original image signal regardless of if the grid is used or not, which is not limited to a specific body part. Another advantage includes its application to any product because the degree of restoration may be easily adjusted according to the type and thickness of the scintillator.

In this comparison study of chest radiography with or without TRUVIEW ART algorithm on anatomic regions, readers preferred the TRUVIEW ART algorithm applied chest radiography to original chest radiography in all 10 anatomic regions and overall appearance.

The retrocardiac and subdiaphragmatic lungs revealed the lowest preference among readers, which was thought to be counterintuitive at first. Scattered radiation degrades the image quality of these areas of obscured lung and, therefore, contrast in these areas may be restored by using a grid. A phantom study revealed similar results with software-based scatter correction by demonstrating greater contrast improvement in the heart and abdominal areas than the lung area (9). In comparison, the areas of the thoracic spine and azygoesophageal recess, of which considerable scattered radiation occurs, received the highest preference for the algorithm-applied image. The difference of the current approach from the grid imaging or grid-like software-based scatter correction is that the scatter correction occurred before the object. Therefore, the corrected signal is irrespective of scattered radiation generated by anatomic structures. Our results reveal that the current approach is more effective in high contrast areas such as the thoracic spine or unobscured lung than areas of relatively low contrast such as retrocardiac lung or subdiaphragmatic lung. Interestingly, the azygoesophageal recess revealed high preference despite being an obscured lung. A potential explanation for this observation would be that the affected part of the lung is small and the preference is affected by surrounding structures such as increased sharpness of the spine.

The unobscured lung, which occupied the largest area of the whole chest radiograph, revealed a high preference value of 3.8. Thus, this may have affected the high preference of the overall appearance, and the TRUVIEW ART algorithm is considered to have clinical significance in improving the overall chest radiographic image quality. Interestingly, the unobscured lung is most likely to have two points as well as five points, so the effect of reducing the scattering using the TRUEVIEW ART algorithm have various effects on unobscured lungs compared to other anatomic areas.

There are several limitations in the TRUVIEW ART algorithm as well. First, the noise included in the acquired image will be also emphasized. Therefore, the automatic exposure control of the X-ray system has to be used or proper irradiation condition should be considered. Second, since this technique requires repetitive searching and calculation time during the image restoration process, it is necessary to optimize the image restoration algorithm for real-time processing. Last, because the difference between two images with or without TRUVIEW ART algorithm are so conspicuous, the readers could distinguish them easily, although the readers were blinded to technical factors of them. Thus, further receiver operating characteristic studies with a larger number of images are necessary to compare the diagnostic accuracy of chest radiograph images with or without TRUVIEW ART algorithm.

In conclusion, the chest radiography image quality with TRUVIEW ART algorithm is superior to original chest radiography in all of the anatomical regions. This new technique could improve the sharpness of the image, and could be appropriately applied for clinical use.

Supplementary Materials

The online-only Data Supplement is available with this article at https://doi.org/10.3348/kjr.2018.19.1.147.

REFERENCES

1. Lee DL, Cheung LK, Rodricks BG, Powell GF. Improved imaging performance of a 14"x17" direct radiography system using a se/tft detector. Proc. *SPIE* 1998:14-23
2. Zhao W, Blevis I, Germann S, Rowlands JA, Waechter D, Huang Z. Digital radiology using active matrix readout of amorphous selenium: construction and evaluation of a prototype real-time detector. *Med Phys* 1997;24:1834-1843
3. Siewerdsen JH, Antonuk LE, el-Mohri Y, Yorkston J, Huang W, Boudry JM, et al. Empirical and theoretical investigation of the noise performance of indirect detection, active matrix flat-panel imagers (AMFPIs) for diagnostic radiology. *Med Phys* 1997;24:71-89
4. Colbeth RE, Cooper VN, Gilblom DL, Harris RA, Job ID, Klausmeier-Brown ME, et al. Characterization of a third-generation multimode sensor panel. Proc. *SPIE* 1999:491-500
5. Samei E, Flynn MJ. An experimental comparison of detector performance for direct and indirect digital radiography systems. *Med Phys* 2003;30:608-622
6. Fish DA, Brinicombe AM, Pike ER, Walker JG. Blind deconvolution by means of the Richardson-Lucy algorithm. *J Opt Soc Am A* 1995;12:58-65
7. Levin A, Fergus R, Durand F, Freeman WT. Deconvolution using natural image priors. Massachusetts Institute of Technology, Computer Science and Artificial Intelligence Laboratory. https://groups.csail.mit.edu/graphics/CodedAperture/SparseDeconv-LevinEtAl07.pdf. Published January, 2007. Accessed May 12, 2017.
8. Peng-Xiang J, Feng Z, Bin Y, Shang-Lian B. Scattering correction method for panel detector based cone beam computed tomography system. *Chinese Physics B* 2010;19:087802
9. Mentrup D, Jockel S, Menser B, Neitzel U. Iterative scatter correction for grid-less bedside chest radiography: performance for a chest phantom. *Radiat Prot Dosimetry* 2016;169:308-312
10. Renger B, Brieskorn C, Toth V, Mentrup D, Jockel S, Lohöfer F, et al. Evaluation of dose reduction potentials of a novel scatter correction software for bedside chest x-ray imaging. *Radiat Prot Dosimetry* 2016;169:60-67